Available online at www.sciencedirect.com
SCIENCE @ DIRECT®

ELSEVIER

Earth and Planetary Science Letters 247 (2006) 157–170

EPSL

www.elsevier.com/locate/epsl

# Seismic anisotropy beneath the Northern Apennines (Italy): Mantle flow or lithosphere fabric?

J. Plomerová [a,*], L. Margheriti [b], J. Park [c], V. Babuška [a], S. Pondrelli [b], L. Vecsey [a], D. Piccinini [b], V. Levin [d], P. Baccheschi [b], S. Salimbeni [b]

[a] *Geophysical Institute, Czech Acad. of Sci., Boční II, 141 31 Prague 4, Czech Republic*
[b] *Istituto Nazionale di Geofisica e Vulcanologia, Italy*
[c] *Yale University, Department of Geology and Geophysics, New Haven, USA*
[d] *Rutgers University, Department of Geological Sciences, NJ, USA*

Received 30 June 2005; received in revised form 14 April 2006; accepted 17 April 2006
Available online 6 June 2006
Editor: Scott King

**Abstract**

Shear-wave splitting estimates from recordings of 10 portable seismographic stations during the first year of the RETREAT seismic deployment, in combination with broadband data from the Italian national seismic network, are associated with seismic anisotropy within the upper mantle beneath the Northern Apennines. Anisotropic parameters derived from both shear-wave splitting and P travel-time residuals vary geographically and depend on event back-azimuth, reflecting complexity in the underlying mantle strain field. Variations of the splitting time delays and fast polarization seem to exclude a 2-D sublithosphere corner flow, associated with the Apennines subduction, as the main source of the inferred anisotropy. The anisotropic signal may be generated by a frozen-in fabric of the Adriatic and Tyrrhenian lithosphere domains, or by flow variations induced by episodic and fragmentary slab rollback.


*Keywords:* SKS birefringence; seismic anisotropy; continental dynamics; Northern Apennines

## 1. Introduction

The Apennine fold and thrust belt developed from the latest Cretaceous to early Pleistocene at the subduction-collisional boundary between the European and the westward subducted Adriatic and Ionian microplates [1–3]. The chain developed through the deformation of major palaeogeographic internal domains (tectono-sedimentary sequences of the Ligurian-Piedmont Ocean) and external domains (sedimentary sequences derived from the deformation of the continental Adria passive margin). From the late Miocene, the geometry of the thrust belt was strongly modified by extensional faulting, volcanic activity, crustal thinning and formation of oceanic crust correlated with the development of the Tyrrhenian Basin [4,5].

Since that time, the Apennine orogeny has been paired with simultaneous extension in the Tyrrhenian Sea and, in general, eastward slab rollback of the subducting Adriatic plate, as a part of the ongoing collision of the Eurasian and African plates [5,6]. In other words, the contact of the Tyrrhenian (over-riding) retro-plate and the Adriatic pro-plate moves in the direction opposite to

* Corresponding author. Fax: +420 272761549.
*E-mail address:* jpl@ig.cas.cz (J. Plomerová).

0012-821X/$ - see front matter © 2006 Elsevier B.V. All rights reserved.
doi:10.1016/j.epsl.2006.04.023

convergence at the subduction zone, and it is often denoted as “trench retreat”. The Apennines orogen is largely continuous along its strike from Liguria in the north to Calabria in the south, suggesting a similarly continuous mantle process beneath the orogen. If subduction and trench retreat are ongoing processes in the Northern Apennines, the seismic hazard of central Italy would be much greater than suggested by the modest level of 20th century seismic activity. The scarcity of large earthquakes in the historical record (roughly 2500 yr) has motivated hypotheses that subduction is not a steady-state process. Faccenna et al. [5] argue that past subduction in the Apennines convergence zone has occurred at rates as large as 5 cm/yr during isolated episodes since 30 Ma, but current motion is much smaller, if not absent [7,8]. Wortel and Spakman [9] argue that portions of the Apennines slab have begun to detach from the surface plate. A study of mantle anisotropy by the multidisciplinary project RETREAT (REtreating-TRench, Extension and Accretion Tectonics) aims at developing a self-consistent dynamic model of syn-convergent extension in the Northern Apennines [10]. If Apennines uplift can be modelled as a consequence of a steady subduction process, details of the 2-D mantle flow will help constrain the lower boundary conditions of the deforming crust. If subduction has halted or the slab has begun to founder, a 3-D mantle flow pattern may have developed. Finally, because continental lithosphere often preserves mantle fabrics from its formation, fossil anisotropy may be substantial [13,14].

Lithosphere on both sides of the orogen is continental, so parallels with typical subduction zones must use analogies. The Northern Apennine orogen occupies a position usual for forearc orogenic belts in ocean–continent subduction settings, such as the Olympics Mountains in Cascadia and Nias Island offshore Sumatra. The Northern Apennines are composed largely of accumulated sediments and metasedimentary rocks. The Po River valley of northern Italy and the Adriatic Sea occupies the position of the offshore trench. The subducting Adriatic pro-plate is identified to the northeast of the Apennines orogen, underlying an uncertain fraction of the Adriatic Sea. The complicated geometry of Adriatic plate subduction [9–12] suggests that the formerly continuous Apennines–Maghrebides subduction is now fragmented along the Italian peninsula in two arcuate orogenic segments: the Northern Apennines (NA) and the Calabrian Arc (CA). The Calabrian Arc still exhibits many features of an active subduction zone, including arc volcanism in the Aeolian Islands and deep seismicity down to 600 km. The Northern Apennines lacks both these features. Its high wavespeed feature imaged in tomographic studies may represent stalled subduction or lithospheric detachment.

Although much of Apennines tectonics may arise from crustal processes, deformation in the underlying mantle likely determines the overall orogenic setting. The distribution of seismic anisotropy in the upper mantle, the crust and lithosphere thicknesses, and the location and geometry of the Adriatic slab should help define mantle dynamics in the region, and are specific objectives of the RETREAT project in the Northern Apennines (Fig. 1). The RETREAT seismic array covers the Northern Apennines (NA) of central Italy, including bordering areas of Liguria, the Apuane Alps and the southern Po River plain (Fig. 1). The temporary deployment started operation in October 2003 with 10 broadband stations, augmented by permanent observatories of the Istituto Nazionale di Geofisica e Vulcanologia (INGV).

Large-scale seismic anisotropy in a peridotite mantle is due primarily to olivine lattice preferred orientation (LPO). LPO anisotropy can arise from fossil rock textures in the continental mantle lithosphere [13,14] and from present-day sublithosphere mantle flow (e.g., [15,16]). Plate subduction and slab retreat can induce mantle flow that is very complicated [17,18], e.g., due to flow around slab margins or through a slab window [19,20]. To investigate the upper mantle, we estimate body-wave anisotropic parameters—shear-wave splitting and P-residual spheres. To analyze splitting, we use seismic data from portable broadband stations, as well as from permanent three-component INGV observatories. P-wave anisotropy has been the subject of previous studies [21–23]. These use larger datasets than available from the initial year of the RETREAT deployment, albeit largely with single-component high-frequency data. Each shear-wave splitting measurement integrates a vertical profile beneath the observing station. Because multiple crossing raypaths are not critical to the interpretation, an analysis of the RETREAT dataset after a single year’s deployment can resolve important structural issues.

Previous measurements of azimuthal variability in shear-wave splitting at 10-station Northern Apennines Profile (NAP) in 1994, south of the RETREAT array, have been interpreted in terms of compressional tectonics involving at least the entire subducting lithosphere [24], or of mantle flow due to the subduction of Adriatic pro-plate [25–27]. Orogen-parallel fast polarization at the Apennines crest was observed to rotate to orogen-normal on the Tyrrhenian side, suggesting a transition from trench-parallel mantle flow associated with slab deformation and rollback to upper mantle extension associated with back-arc spreading [28]. The extensional Lau Basin behind the Tonga subduction zone shows similar splitting behaviour [29]. This effect has been modeled by Hall et al. [30], but different results are found in other subduction contexts [31–33].

Mantle xenoliths close to the NAP deployment show well-developed LPO [34], though samples are scarce, small and restricted to the Torre Alfina area (see Fig. 3). If the orogen-parallel splitting [24–26] of some NAP stations continued northwest along the Apennines, this would be strong evidence for a 2-D mantle flow associated with the subduction and rollback of the Adriatic proplate. However, variations in initial RETREAT splitting results suggest either an influence of pre-existing lithosphere mantle fabric or a 3-D mantle flow in the sublithospheric mantle. Using shear-wave birefringence and the direction dependence of P travel-time residuals, we can characterize these two possibilities in the broad features of upper mantle anisotropy beneath the Northern Apennines.

## 2. Shear-wave anisotropy

Seismic stations in Italy receive core-refracted shear waves from a variety of back-azimuths. We analyzed shear-wave birefringence with several methods [35–37] to check the self-consistency of our dataset. We report results mainly from strong earthquakes (magnitude $M>6$) analyzed with the method employed by Šílený and Plomerová [36]. We evaluate the fast polarization strike and time delay between slow and fast waves in rotated LQT coordinates, so that information from vertical motion is included. Data are typically bandpass-filtered to 3–30 s before analysis. We minimize energy on the transverse component (Fig. 2) and apply a bootstrap estimate of variance for the splitting parameters [37]. We apply a stringent stability test on the splitting parameters, in which we require the fast polarization to remain stable to random noise fluctuations.

Time delays for robustly determined birefringence vary between 0.7 and 2 s, with a typical delay of 1.2 s (Fig. 3

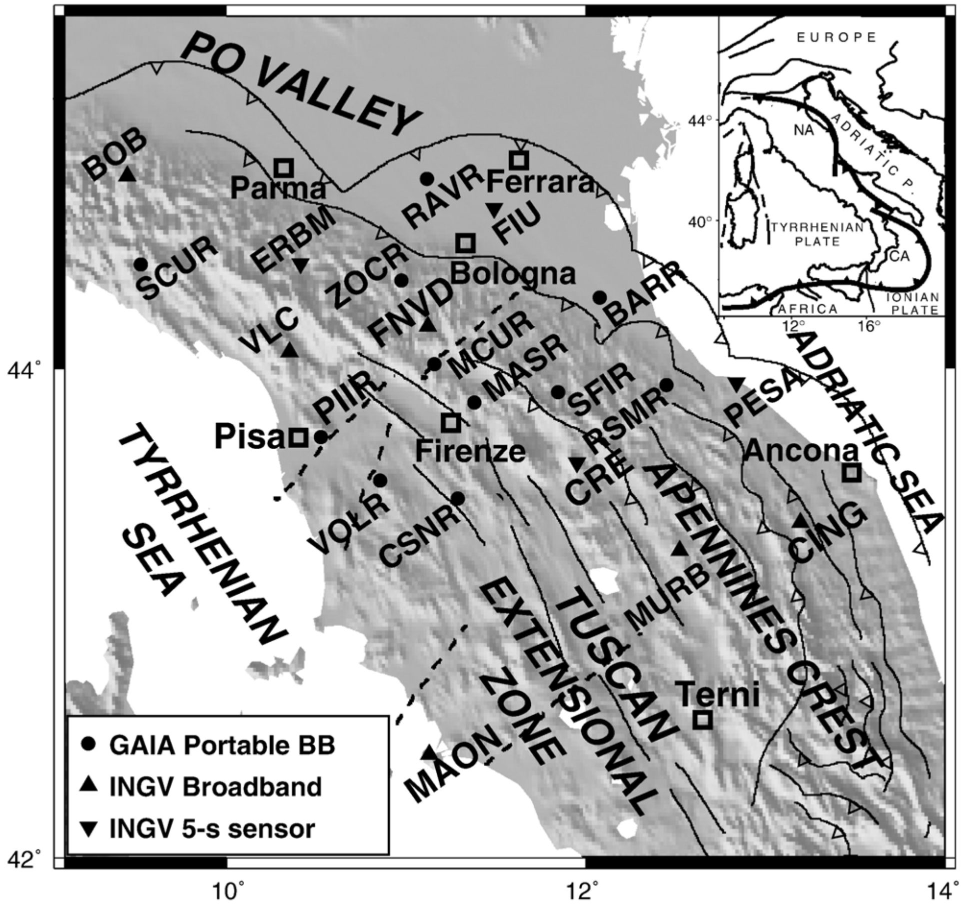


Fig. 1. Relief map of the RETREAT field area in central Italy with seismographic stations used in this study.

and Table 1). For mantle peridotite with 4% Vs anisotropy and a mean Vs = 4.4 km/s, a 1.2-s splitting delay would be generated in a layer 130 km thick, assuming a horizontal 'fast' symmetry axis. However, birefringence varies greatly in the region and many observed SKS waves deviated from simple birefringence patterns. Although the signal level of most seismograms in our dataset was good, a large proportion of SKS phases failed one or

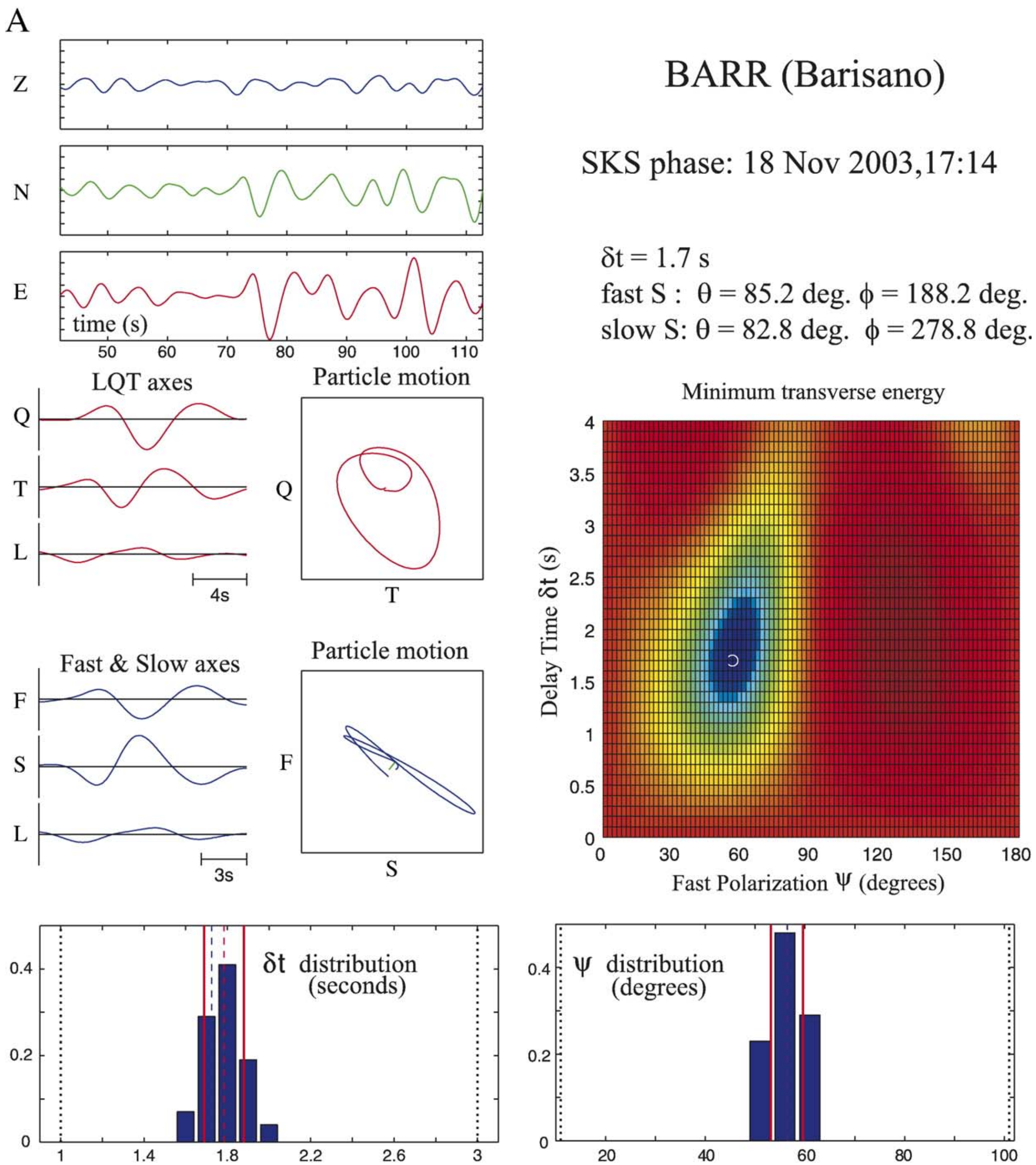


Fig. 2. Examples of shear-wave splitting parameters evaluated (A) at station BARR in the Po Plain and (B) at stations ZOCR, located within the orogenic wedge and PIIR in the extensional Tyrrhenian plate. Splitting of shear waveforms of the same event with back-azimuth 64° is shown. The SKS phase splits at stations BARR and ZOCR with the time delays of 1.7 s and 1.5 s, whereas the null split was evaluated at station PIIR. Standard deviations of the splitting parameters are determined by the bootstrap method [37].

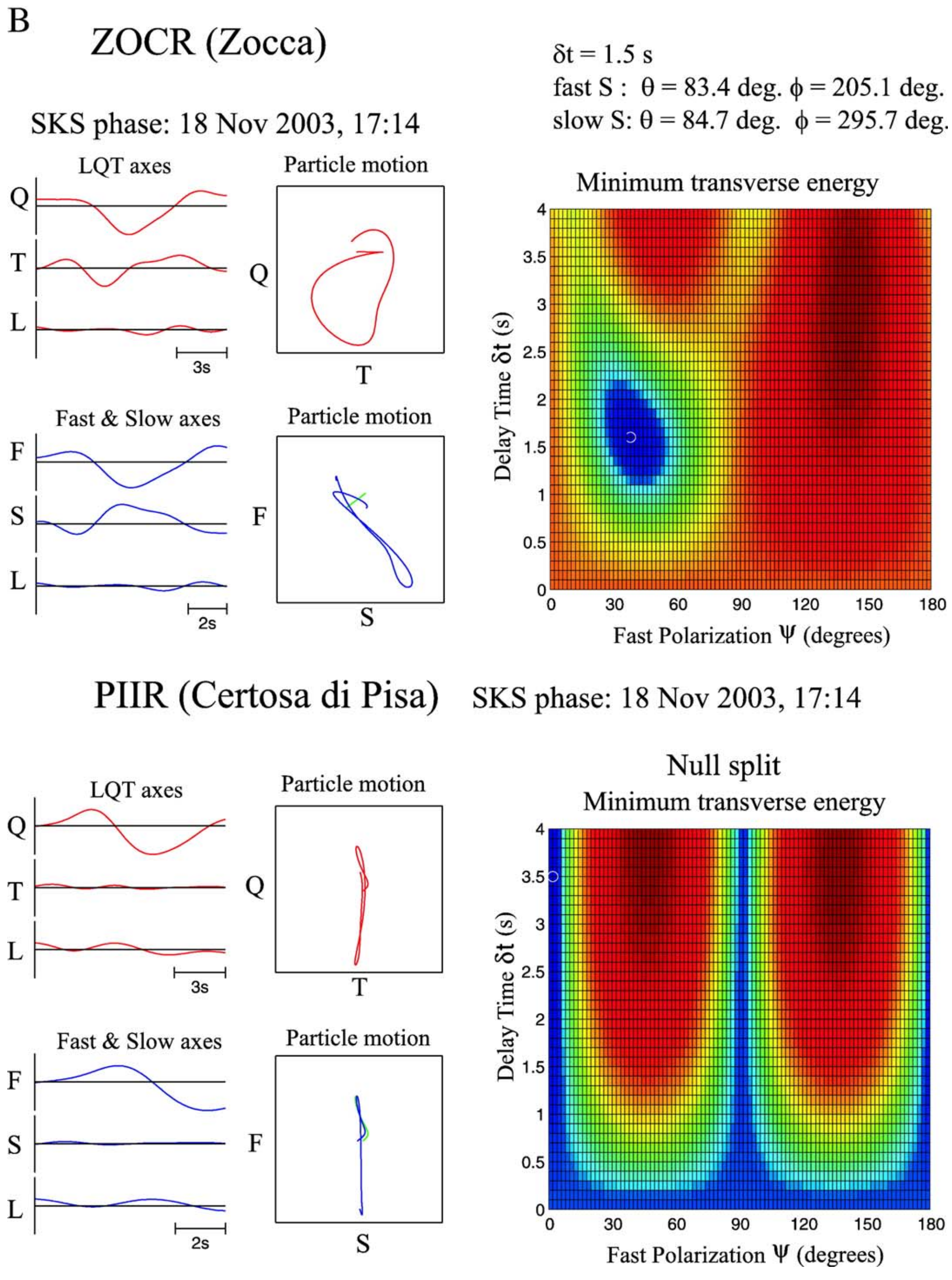


Fig. 2 (*continued*).

more criteria for a stable estimate of anisotropic parameters. In addition, many of the stable birefringence estimates returned no splitting (circles in Fig. 3).

Splitting parameters depend on back-azimuth and incidence angle of the incoming shear waves if anisotropic properties of the upper mantle vary with depth or laterally, or else if anisotropic symmetry axes are inclined. By grouping the RETREAT dataset into events from the west and events from the northeast, we contrast paths that arrive from the Adriatic, or pro-plate, side of the

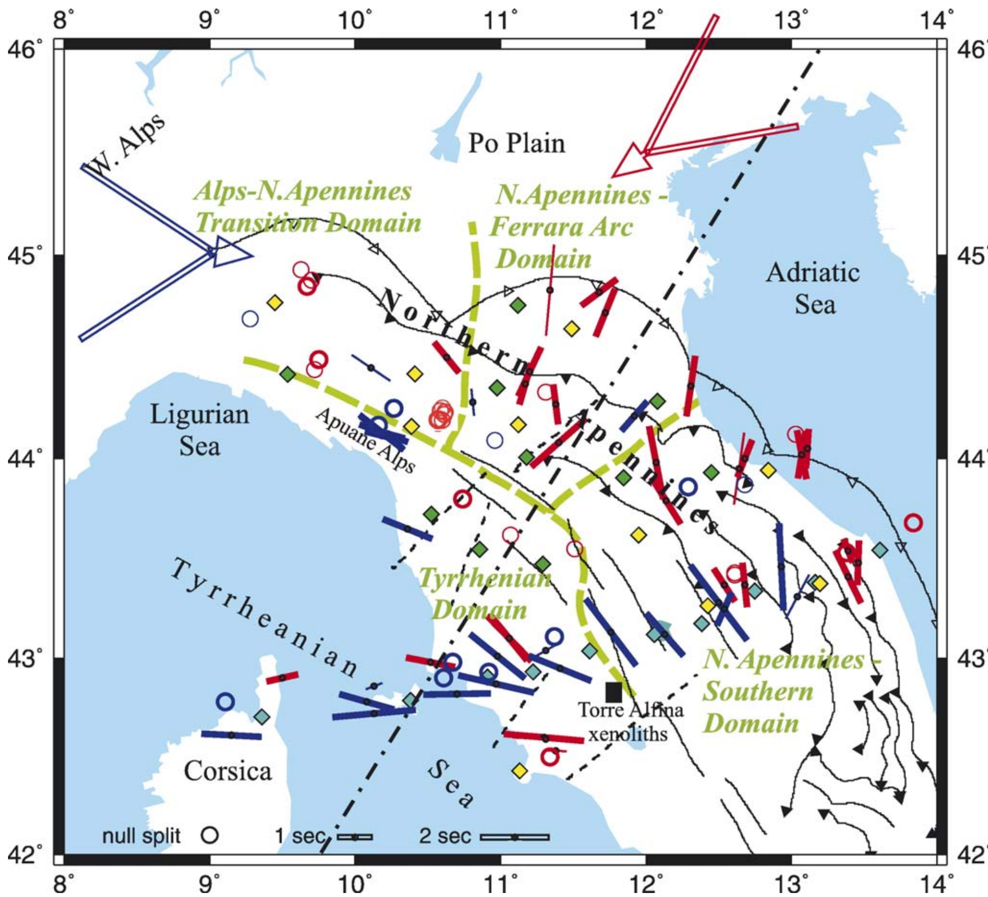


Fig. 3. Shear-wave birefringence estimates for teleseismic data recorded by the temporary RETREAT deployment (green diamonds), at INGV permanent stations (yellow diamonds) and the NAP (North Apennine Profile—blue diamonds, [24]), plotted at piercing points at a depth of 100 km. The big arrows on the top mark the SW–NW (blue) and NE (red) fans of azimuths of arriving shear waves. Dashed green curve marks labelled terrane boundaries as deduced from the variations of the splitting parameters. The dot-dashed line locates the cross-sections of Fig. 5.

Apennines orogen with paths that arrive from the Tyrrhenian, or retro-plate, side. The birefringence of shear waves that arrive from the Adriatic pro-plate, or downgoing, side differs from the Tyrrhenian retro-plate, or overriding, side. Fig. 3 plots the fast polarizations of split shear waves of these two groups respectively with red and blue colours highlighting these differences. The birefringence estimator [36] scales the fast shear-wave polarization inclination with the SKS incidence angle, which is helpful in some situations. For comparison of the RETREAT dataset with previous results on azimuthal anisotropy in the Northern Apennines [25], however, we show only the fast polarization azimuths in Fig. 3.

We distinguish several regions that we refer to as “domains” (Fig. 3) based on splitting characteristics. Slab-normal fast polarization is common in the centre of our field area in the buried Ferrara arc domain but shows an azimuthal dependence. Strong splitting from the northeast contrasts with weak splitting from the west. Fast polarization trends toward slab-parallel in the southern part of the deployment. Null splits occur throughout the Tuscan extensional region for core-refracted shear waves arriving from the northeast. Null or unstable splits from the northeast are also seen in splitting measurements from MEDNET (INGV) station VLC, which lies in the extensional region. For western back-azimuths, the VLC splitting behaves similar to RETREAT station PIIR (Certosa di Pisa, see also Fig. 5) with predominantly NW–SE fast polarization subparallel to the orogen trend. This polarization trends smoothly into the fast shear-wave polarizations in the Tyrrhenian region recorded in 1994 by the western part of the NAP array and confirmed by MAO station measurements (Table 1). The splitting in this domain is direction sensitive for both RETREAT and NAP datasets, e.g., along the NAP line null splits were observed for the WNW back-azimuths. By contrast, we measured null splitting for two stations in the northwest of the RETREAT deployment (station SCUR and nearby INGV

Table 1
Shear-wave splitting at RETREAT array in the Northern Apennines, shown in Fig. 2

| Station name | Station lat. (°N) | Station long. (°E) | Event date YYMMDD | Hypo. lat. (°) | Hypo. long. (°) | Hypo. depth (km) | BAZ (°) | $\phi$ (°) | d$\phi$ (°) | $\delta t$ (s) | d$\delta\tau$ (s) |
|---|---|---|---|---|---|---|---|---|---|---|---|
| BARR | 44.2828 | 12.0797 | 031118 | 12.025 | 125.416 | 35 | 65 | 188 | 3 | 1.7 | 0.1 |
| BARR | 44.2828 | 12.0797 | 040503 | −37.649 | −73.439 | 21 | 240 | 41 | 10 | 1.1 | 0.4 |
| CSNR | 43.47311 | 11.29017 | 031118 | 12.025 | 125.416 | 35 | 64 | – | – | Null | – |
| MCUR | 44.0050 | 11.1797 | 031118 | 12.025 | 125.416 | 35 | 64 | 228 | 2 | 2.1 | 0.2 |
| PIIR | 43.7219 | 10.5250 | 031118 | 12.025 | 125.416 | 35 | 64 | – | – | Null | – |
| PIIR | 43.7219 | 10.5250 | 040503 | −37.649 | −73.439 | 21 | 240 | 112 | 10 | 1.5 | 0.3 |
| RAVR | 44.75587 | 11.11880 | 031118 | 12.025 | 125.416 | 35 | 64 | 185 | 2 | 2.7 | 0.1 |
| RSMR | 43.9303 | 12.4497 | 031118 | 12.025 | 125.416 | 35 | 65 | 201 | 9 | 1.1 | 0.2 |
| RSMR | 43.9303 | 12.4497 | 040503 | −37.649 | −73.439 | 21 | 240 | – | – | Null | – |
| RSMR | 43.9303 | 12.4497 | 040423 | −9.275 | 122.807 | 71 | 80 | 188 | 2 | 2.1 | 0.3 |
| SCUR | 44.4156 | 9.5361 | 031118 | 12.025 | 125.416 | 35 | 63 | – | – | Null | – |
| SCUR | 44.4156 | 9.5361 | 040423 | −9.275 | 122.807 | 71 | 80 | – | – | Null | – |
| SFIR | 43.90477 | 11.84695 | 031118 | 12.025 | 125.416 | 35 | 65 | 169 | 3 | 2.1 | 0.2 |
| VOLR | 43.54778 | 10.8572 | 031118 | 12.025 | 125.416 | 35 | 64 | – | – | Null | – |
| ZOCR | 44.35085 | 10.97650 | 031118 | 12.025 | 125.416 | 35 | 64 | 205 | 3 | 1.5 | 0.1 |
| ZOCR | 44.35085 | 10.97650 | 040503 | −37.649 | −73.439 | 21 | 240 | 354 | 26 | 0.8 | 0.6 |
| ZOCR | 44.35085 | 10.97650 | 040423 | −9.275 | 122.807 | 71 | 80 | 196 | 7 | 1.2 | 0.2 |
| BOB | 44.7679 | 9.4478 | 031031 | 37.812 | 142.619 | 10 | 35 | – | – | Null | – |
| BOB | 44.7679 | 9.4478 | 031118 | 12.025 | 125.416 | 35 | 63 | – | – | Null | – |
| BOB | 44.7679 | 9.4478 | 031210 | 23.039 | 121.362 | 10 | 59 | – | – | Null | – |
| BOB | 44.7679 | 9.4478 | 040529 | 34.3 | 141.33 | 38 | 38 | – | – | Null | – |
| CING | 43.3756 | 13.1954 | 040128 | −3.12 | 127.4 | 17 | 75 | −26 | 6 | 1.64 | 1.0 |
| CING | 43.3756 | 13.1954 | 040403 | 36.428 | 141.008 | 31 | 40 | −21 | 18 | 0.68 | 1.0 |
| CING | 43.3756 | 13.1954 | 040503 | −37.649 | −73.439 | 21 | 239 | 28 | 18 | 1.44 | 1.0 |
| CING | 43.3756 | 13.1954 | 040519 | 22.62 | 121.45 | 20 | 61 | 2 | 5 | 1.24 | 0.2 |
| CING | 43.3756 | 13.1954 | 040529 | 34.3 | 141.33 | 38 | 41 | – | – | Null | – |
| CRE | 43.6188 | 11.9516 | 040403 | 36.428 | 141.008 | 31 | 39 | −32 | 6 | 1.55 | 0.3 |
| ERBM | 44.4194 | 10.4126 | 031118 | 12.025 | 125.416 | 35 | 64 | −39 | 18 | 1.10 | 1.0 |
| ERBM | 44.4194 | 10.4126 | 031225 | −22.252 | 169.488 | 10 | 278 | −56 | 10 | 1.35 | 0.3 |
| FIU | 44.6403 | 11.4916 | 031031 | 37.812 | 142.619 | 10 | 37 | 53 | 8 | 1.25 | 0.5 |
| FIU | 44.6403 | 11.4916 | 031118 | 12.025 | 125.416 | 35 | 65 | 22 | 2 | 1.45 | 0.1 |
| FNVD | 44.16782 | 11.1229 | 040503 | −37.649 | 73.439 | 21 | 238 | – | – | Null | – |
| FNVD | 44.16782 | 11.1229 | 040519 | 22.62 | 121.45 | 20 | 60 | −7 | 6 | 1.12 | 0.2 |
| FNVD | 44.16782 | 11.1229 | 040529 | 34.3 | 141.33 | 38 | 39 | – | – | Null | – |
| MAON | 42.4283 | 11.1309 | 031031 | 37.812 | 142.619 | 10 | 36 | −85 | 6 | 2.28 | 0.3 |
| MAON | 42.4283 | 11.1309 | 031118 | 12.025 | 125.416 | 35 | 65 | – | – | Null | – |
| MAON | 42.4283 | 11.1309 | 031210 | 23.039 | 121.362 | 10 | 60 | −88 | 10 | 0.64 | 0.8 |
| MAON | 42.4283 | 11.1309 | 040403 | 36.428 | 141.008 | 31 | 38 | −87 | 13 | 1.92 | 0.7 |
| MURB | 43.263 | 12.4256 | 040403 | 36.428 | 141.008 | 31 | 39 | – | – | Null | – |
| MURB | 43.263 | 12.4256 | 040519 | 22.62 | 121.45 | 20 | 61 | −6 | 4 | 1.24 | 0.2 |
| MURB | 43.263 | 12.4256 | 040529 | 34.3 | 141.33 | 38 | 40 | – | – | Null | – |
| PESA | 43.941 | 12.840 | 031031 | 37.812 | 142.619 | 10 | 38 | – | – | Null | – |
| PESA | 43.941 | 12.840 | 031118 | 12.025 | 125.416 | 35 | 66 | 9 | 2 | 1.35 | 0.1 |
| PESA | 43.941 | 12.840 | 040503 | −37.649 | 73.439 | 21 | 239 | – | – | Null | – |
| PESA | 43.941 | 12.840 | 040519 | 22.62 | 121.45 | 20 | 61 | 4 | 4 | 1.10 | 0.2 |
| VLC | 44.1591 | 10.3862 | 010626 | −17.745 | −71.649 | 24 | 251 | −46 | 10 | 1.07 | 0.5 |
| VLC | 44.1591 | 10.3862 | 010703 | 21.641 | 142.984 | 290 | 44 | – | – | Null | – |
| VLC | 44.1591 | 10.3862 | 010705 | −16.086 | −73.987 | 62 | 254 | −83 | 5 | 1.04 | 0.4 |
| VLC | 44.1591 | 10.3862 | 010707 | −17.543 | −72.077 | 33 | 252 | −73 | 10 | 1.03 | 0.4 |
| VLC | 44.1591 | 10.3862 | 010907 | −13.166 | 97.297 | 10 | 101 | – | – | Null | – |
| VLC | 44.1591 | 10.3862 | 011012 | 12.686 | 144.980 | 37 | 48 | – | – | Null | – |
| VLC | 44.1591 | 10.3862 | 011019 | −4.102 | 123.907 | 33 | 76 | – | – | Null | – |
| VLC | 44.1591 | 10.3862 | 011218 | 23.954 | 122.734 | 14 | 58 | – | – | Null | – |
| VLC | 44.1591 | 10.3862 | 020305 | 6.033 | 124.249 | 31 | 69 | – | – | Null | – |
| VLC | 44.1591 | 10.3862 | 020814 | 14.101 | 146.199 | 30 | 57 | – | – | Null | – |

(continued on next page)

Table 1 (*continued*)

| Station name | Station lat. (°N) | Station long. (°E) | Event date YYMMDD | Hypo. lat. (°) | Hypo. long. (°) | Hypo. depth (km) | BAZ (°) | $\phi$ (°) | d$\phi$ (°) | $\delta t$ (s) | d$\delta\tau$ (s) |
|---|---|---|---|---|---|---|---|---|---|---|---|
| VLC | 44.1591 | 10.3862 | 021012 | −8.295 | −71.738 | 534 | 258 | −27 | 4 | 1.07 | 0.3 |
| VLC | 44.1591 | 10.3862 | 030122 | 18.770 | −104.104 | 24 | 300 | – | – | Null | – |
| VLC | 44.1591 | 10.3862 | 030310 | 1.692 | 127.296 | 93 | 69 | – | – | Null | – |
| VLC | 44.1591 | 10.3862 | 030526 | 38.849 | 141.568 | 68 | 36 | – | – | Null | – |
| VLC | 44.1591 | 10.3862 | 030526 | 2.354 | 128.855 | 31 | 67 | – | – | Null | – |
| VLC | 44.1591 | 10.3862 | 030620 | −30.608 | −71.637 | 33 | 242 | −42 | 10 | 1.04 | 0.5 |
| VLC | 44.1591 | 10.3862 | 031118 | 12.025 | 125.416 | 35 | 64 | – | – | Null | – |
| VLC | 44.1591 | 10.3862 | 040207 | −4.003 | 135.023 | 10 | 81 | – | – | Null | – |
| VLC | 44.1591 | 10.3862 | 040423 | −9.362 | 122.839 | 65 | 80 | – | – | Null | – |

station BOB to the north) for both the SW and NE back-azimuths (see also Table 1). These stations straddle the regional transition from the Apennines to the western Alps, a transition evident in P-residual analysis (see Section 3 and Fig. 4).

Details of the birefringence estimates confirm the likely complexity of the anisotropy beneath the Apennines. We found some frequency dependence in the anisotropic parameters, which Rumpker et al. [38], Matcham et al. [39] and Marson-Pidgeon and Savage [40] associate with a vertically varying anisotropy. We tested a simpler birefringence estimator, based on cross-correlation, that does not test for stability. For this estimator, many more core-refracted shear waves appear to be split, but the variance of splitting parameters is much larger, e.g., some time delays as large as 3 s are obtained. In an independent analysis of 3 yr of data for MEDNET station VLC with the method described by Menke and Levin [41], only nine stable birefringence estimates were obtained, with only two of these from the data-rich northeast back-azimuth sector. Attempts to model all nine splitting estimates with a single model returned fast polarization for VLC at 124° strike with 1.2-s time delay, a value similar to that obtained for four single records using the [36] estimator (Table 1). Attempts to fit splitting parameters at station VLC with a two-layer anisotropic model failed to improve substantially a one-layer model, suggesting that the back-azimuth variation is caused by 3-D anisotropic structure and not by a 1-D layered model.

Complex splitting seems to exclude a simple 2-D sublithosphere mantle flow as the main source of anisotropy. There are geographical variations among the robust birefringence time delay and fast polarization estimates (Fig. 3), but the pattern of variation in the southern part of the array exhibits continuity with splitting parameters derived from the 1994 North Apennine Profile (NAP) as reported by Margheriti et al. [24]. This earlier study derived parameters both via covariance matrix decomposition and a cross-correlation algorithm from a collection of events and found similar averaged splitting measurements. Rough agreement for splitting parameters from independent datasets (NAP and the southern part of RETREAT) and varying splitting estimators argues that the strong lateral variations reflect underlying structure and not data problems.

## 3. P-wave anisotropy

Careful processing of the P travel-time residuals, which minimizes effects of distant heterogeneities and isolates relative velocity variations beneath a station [21], can reveal directional P-velocity variations, which can be compared with shear-wave anisotropic parameters. P residuals also are the datasets used in regional tomography studies, so an interpretation of P anisotropy often implies a trade-off with 3-D isotropic structure. Fig. 4 presents the direction-dependent parts of the relative residuals in P-residual spheres [22], plotted in lower hemisphere projection, from which a directional mean of the relative residuals, related to the isotropic velocity variations, is eliminated. The 'bipolar pattern' of the P spheres indicates that waves arrive earlier from one side compared with waves from the opposite side. In the western Alps of northwest Italy, olivine LPO of the mantle lithosphere, characterized by the high-velocity foliations ($a$,$c$) dipping to the east, was inferred by [21] to explain P residuals for stations marked by solid blue triangles in Fig. 4. Stations in the Northern Apennines and to the east (marked by full red triangles in Fig. 4) show high velocities dipping consistently to the SW. Both the Alpine and the Northern Apennine P-residual patterns are independent of normalization, time period and data source, i.e., whether bulletin data (ISC, regional bulletins) or waveform picking [42] were used.

If we interpret the above pattern in terms of lithospheric domains with distinct anisotropic features, stations with an unclear P-residual pattern (yellow triangles

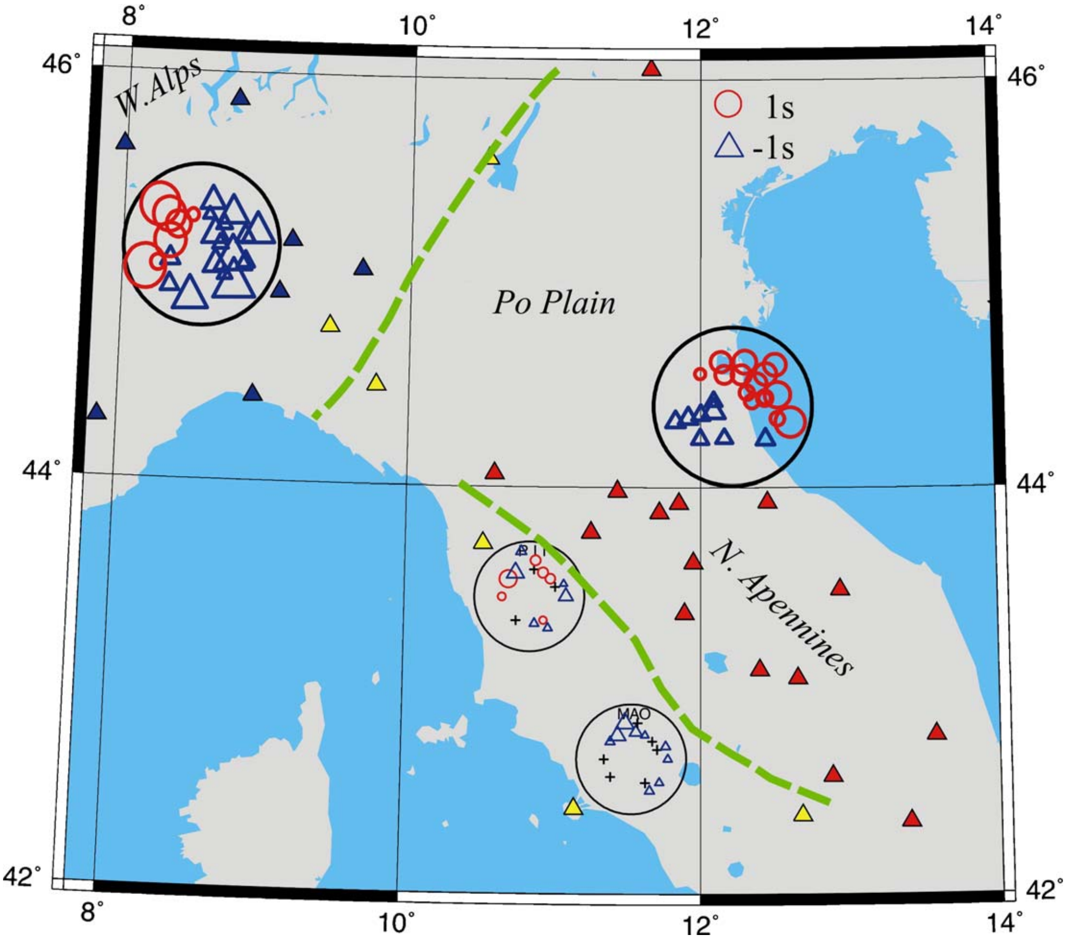


Fig. 4. Travel-time residuals for P-waves observed at stations in north-central Italy [21,22,42]. Stations with the Northern Apennine P-residual pattern (solid red triangles), i.e., with relatively early arrivals from the SW azimuth (blue triangles in the residual spheres—lower hemisphere projection); stations with the Alpine P-residual pattern (solid blue triangles), i.e., with relatively delayed arrivals from the W (red circles in the spheres), and stations with no clear-cut pattern (solid yellow triangles), i.e., with close to zero deviations (crosses). The diagrams with 'zero' deviations are computed from correlated measurements of Lucente et al. [11] and shown for stations PII and MAO. Two large spheres represent the P pattern at the Alpine and NA groups of stations [22]. Size of the signs is proportional to a value of the relative travel-time deviations. The residuals exhibit dependence on event back-azimuth and incidence angle. The dependence is strongly correlated within distinct geographic areas, indicated on the map.

in Fig. 4) would mark a boundary zone between them. This interpretation is supported by several observations of "null" birefringence at these stations (Fig. 3). Hypothetically, the boundary of the Alpine and Apennine lithosphere roots continues from the Ligurian seashore to the NNE through the Po plain [42]. P-residual spheres with no clear-cut pattern at stations on the Tyrrhenian lithosphere (PII, MAO, Fig. 4; data from [11]) suggest that there might be only a weak upper mantle anisotropy, or an anisotropy with horizontal symmetry axis, which does not generate a bipolar P-residual pattern [43].

The use of P-residual spheres to map inclined lithospheric fabrics was developed for regions without an active subduction zone [44]. P-residual analysis has also been used to trace isotropic P wavespeed slab signatures [45], so an isotropic contribution to the patterns in Fig. 4 must be considered. The residual spheres appear to define a patchwork of geographic terranes. A slab-dominated signal is plausible for the centre of the RETREAT field area, but not to the west. A discontinuous slab or a more complex lithospheric downwelling has been hypothesized to explain complexities in the tomographic models derived from P travel-time anomalies in the region (e.g., [9]). Substantial anisotropy in a patchwork of lithospheric domains, with proper orientation, could influence such complexities.

## 4. Joint interpretation of body-wave anisotropy

Though the different types of seismic waves are sensitive to different structures, large-scale upper mantle anisotropy affects all of them. Mantle anisotropy is confirmed by the presence of shear-wave birefringence, so a purely isotropic interpretation of P-wave travel-time residuals must be re-evaluated. Because teleseismic P waves in the Northern Apennines typically arrive with steep incidence, anisotropy with a horizontal symmetry axis would not affect travel-times greatly. The effect of anisotropy with a tilted symmetry axis, however, can be significant [13].

Fig. 5 shows the anisotropic observations evaluated from the body waves together with two different isotropic images of upper mantle velocity perturbations in the RETREAT field area [11,12]. The contrast in mantle structures sampled by different incoming rays is instructive. Both isotropic images of the upper mantle show a high-velocity heterogeneity interpreted as the subducting Adriatic lithosphere. The Lucente et al. model [11] resolves the slab best at depths below 150 km, because teleseismic body-wave tomography has poorer sensitivity to shallow structure. Piromallo and Morelli [12] have much more resolution at shallower depths, particularly 50–150-km depth, because it includes also local and regional phases (e.g., Pn) in the inversion. Short-wavelength variation in SKS splitting argues for a shallow source of anisotropy, where the use of regional P travel-time residuals should give better resolution of the velocity-perturbation image [12]. Fig. 5 shows that these isotropic velocity perturbation models can diverge significantly on individual transects. Although resolution limitations could cause such discrepancies, the presence of shear-wave splitting suggests that anisotropy could also be at fault.

The temporary stations in the first year of the RETREAT deployment can be divided into three groups along the SW–NE profile crossing the Northern Apennines (see Figs. 1 and 3): (1) stations in the extensional region (PIIR, VOLR, CSNR), (2) stations within the orogenic wedge (ZOCR, SFIR, MCUR), and (3) stations in the Apennine foothills (RSMR) and in the Po Plain (RAVR, BARR). Referenced to the P-wave tomographic models, the lateral change along this section in splitting parameters seems to be related to a transition from low- to high-P wavespeed associated with the subducting Adriatic lithosphere (sketched by the purple lines in Fig. 5). Nulls and unstable splits (the ray shown schematically by the red dashed line) are found at the boundary between fast and slow tomographic anomalies, hypothetically at the bend of the subducting lithosphere. Theoretically speaking, null splitting occurs if a shear wave travels through a medium with no anisotropy or propagates parallel to the symmetry axis of an anisotropic medium. Alternatively, the null splits may indicate a cancellation of opposing birefringence signals, either along lithospheric domain boundaries [13,14] or at a mantle-flow transition. Note that SKS arrivals from the northeast that are observed near the crest of the Apennines and in the Ferrara arc domain (see Fig. 3) exhibit orogen-normal fast polarization. During the same observation period, SKS arrivals from the west observed on the Tyrrhenian side of the Apennines exhibit orogen-parallel fast polarization. Both these groups are separated by a zone with null splits. In Fig. 5, the solid red and blue lines, respectively, show how these SKS phases sample the mantle. In general, phases with prevailingly orogen-normal fast polarization propagate through a low-velocity anomaly in the mantle beneath the Apennines slab. During the same observation period, phases with the orogen-parallel fast polarization propagate up the high-velocity body that we interpret as a slab and through the low-velocity wedge above it (Fig. 5B).

Short-wavelength isotropic velocity variations inferred from seismic travel-time tomography can be caused by longer-wavelength anisotropic structures [46,47], because an isotropic inversion of direction-dependent wavespeed typically involves closely spaced volumes of low- and high-velocity rocks. Unlike the shear-wave birefringence, P-wave travel-time residuals are commonly interpreted in terms of 3-D isotropic structure. However, both tomographic slices in Fig. 5 exhibit a strong contrast between a positive slab anomaly beneath the Apennines and a negative wavespeed anomaly beneath the Adriatic proplate. Because there are few seismic stations in the seismically noisy Po Valley and in the Adriatic Sea directly above the anomaly, this velocity contrast is influenced largely by the directionality of P residuals for stations in the Northern Apennines. All or some of the slow anomaly beneath Adria could be an artefact of the baseline velocity chosen for tomographic display, but the geometry of SKS splitting and P-residual spheres also allows the influence of anisotropy with a trench-normal fast axis that plunges SW with the Apennines slab.

Alternatively, if the anisotropy sensed by SKS splitting has a horizontal symmetry axis, then the effect of anisotropy will have a small influence on teleseismic P-wave residuals. In this case, the splitting would reflect anisotropy and the P residuals would reflect isotropic variations [23]. This issue could be resolved with a larger dataset of SKS birefringence estimates, to determine whether their back-azimuth variation can be modeled best by 3-D structure or a dipping symmetry axis or multi-layered structure—see, e.g., the analysis of Margheriti et al. [25] for station AQU in the central Apennines. Although our analysis of station VLC near the Apennines crest did not favor a layered model (see Section 2),

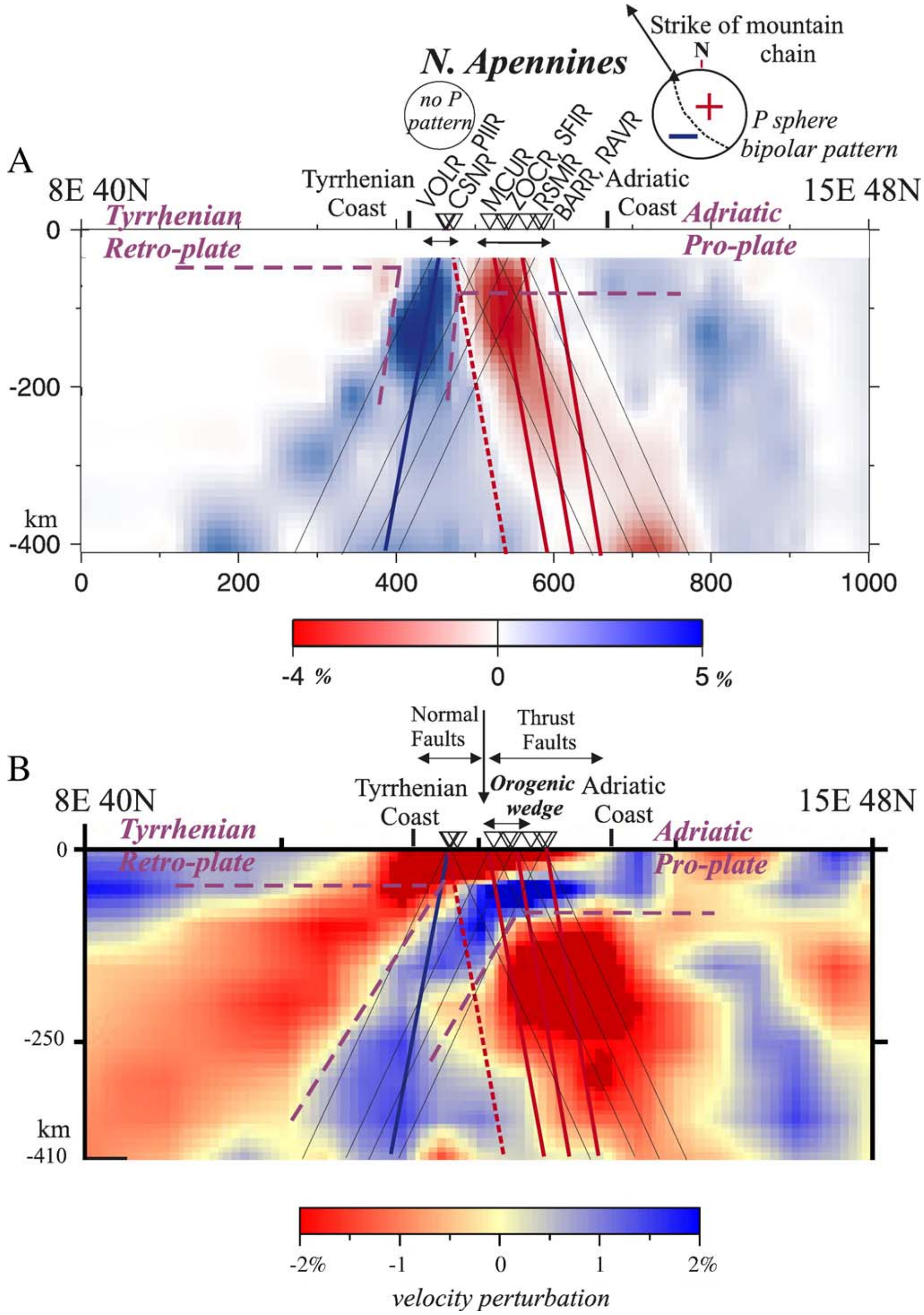


Fig. 5. Selected ray paths for splitting observations plotted against transects of seismic wavespeed anomalies from tomographic models of Italy and surrounding regions. Solid red lines correspond to prevailingly orogen-normal fast polarizations observed from the northeast and solid blue lines to orogen-parallel fast polarizations observed from the west. The dashed red lines correspond to null splits and poorly determined fast polarization observed from the northeast. Black lines mark the most shallow teleseismic P-wave propagation through the tomographic images. Upper (A): colours indicate Vp anomalies (along the 50-km width profile; for its location, see Fig. 3) reported by Lucente et al. [11] from teleseismic body-wave residuals. Lower (B): colours indicate Vp anomalies reported by Piromallo and Morelli [12] from regional and teleseismic travel-time anomalies.

stations that represent the Northern Apennines/Ferrara arc domain have different back-azimuth dependence.

Where S anisotropy exists, P anisotropy can be expected to occur as well, and to have strength at least as large. Strong splitting and large P residuals are found in the Northern Apennines/Ferrara arc domain, and can be jointly interpreted in terms of anisotropy with a dipping axis. Both body-wave types (S and P) localize a region with scarce or null anisotropy in the northwest of the RETREAT deployment, at the transition to the western Alps. In the Tyrrhenian domain, stations exhibit a weak P-residual pattern (Fig. 3), while SKS splitting varies from weak to significantly orogen-parallel (Fig. 4). This suggests the presence of anisotropy with a horizontal symmetry axis in the asthenospheric wedge above the slab and/or in the lithosphere of the overriding Tyrrhenian plate. (In the Tyrrhenian domain, the back-azimuth dependence of splitting would be attributed to 3-D structure, not dipping or multilayered anisotropy.) The correspondence between domains depicted by P spheres and splitting parameters is striking (Figs. 3 and 4) and argues that a mixed anisotropy/isotropy model for the mantle beneath Apennines is required.

Regional Pn velocities in the area [48] can help us constrain the depth of the anisotropic structures, because Pn samples the uppermost mantle beneath the Italian peninsula. Pn propagates mostly subhorizontally, so Pn velocities are sensitive mainly to azimuthal variability of anisotropy within the uppermost mantle, typically shallower than 50-km depth. Mele et al. [48] report orogen-parallel orientation of fast Pn high velocity along the whole Northern Apennines chain, orogen-parallel fast velocity below western Alps and scarce anisotropy beneath the Tyrrhenian basin. Some of these features are corroborated by our data interpretation.

## 5. Discussion

Each of the common models for extension in convergent orogens implies a sublithospheric flow that should be detectable in the pattern of LPO anisotropy. A 2-D slab retreat model can be applied to the shear-wave splitting of the NAP array at the southern edge of the RETREAT deployment [24], in which orogen-normal fast polarization over the Tuscan extensional zone was observed to rotate to orogen-parallel at the crest of the Apennines. Levin et al. [26] found corroborative evidence in receiver functions for an anisotropic fabric at the base of the Adriatic lithosphere aligned with SKS fast polarization near the Apennines crest. A retreating slab would plausibly induce asthenospheric orogen-parallel flow beneath it and orogen-normal extension and crustal thinning above the retro-wedge (supra-slab) mantle. To the south of the NAP profile, Margheriti et al. [25] show that orogen-parallel fast polarization is common for measurements near the Apennines crest and orogen-normal fast polarizations can be found on the Tyrrhenian side of the Apennines. Normal faulting and thin crust characterizes the Tuscan region [49,50], so a continuation of the NAP splitting pattern (and the inferred 2-D mantle flow geometry) to the northwest was anticipated.

The continuation of birefringence measurements to the Northern Apennines, however, reveals different trends. Moving northwest from the NAP profile, our RETREAT observations suggest that fast polarization varies from orogen-parallel to orogen-normal along the Apennines crest. The Tuscan extensional region has weak and back-azimuth sensitive splitting. Nonzero birefringence is measured only for SKS that arrive from the west, for which the fast polarization is orogen-parallel. The interpretations of birefringence in the Northern Apennines are many, but a simple 2-D subduction corner flow is possible only under conditions that seem unlikely. For example, mineralogical variations or the presence of volatiles might cause a varying development of LPO fabric. Since subduction-arc volcanism is absent, the mantle wedge is not likely volatile-rich and we know of no evidence for strong mineralogical variations in the mantle along the Apennines orogen. A 2-D mantle flow fabric could be superimposed within a complex pattern of pre-existing lithospheric fabric. SKS waves on the Tyrrhenian retro-plate side propagate only a short distance within the supra-slab mantle wedge and may acquire their birefringence from anisotropy within the slab. Finally, the mantle flow may be 3-D, suggesting that the Apennines slab is disrupted in this region.

Although subduction is the conventional explanation for Apennine tectonics, modifications and alternatives have been proposed. Evidence for subduction-related mantle flow is best developed in southern Italy, where the generalised SKS splitting measurements suggest asthenospheric flow around the Calabrian slab with a leakage through a slab window in the Sicily channel [19,27]. The complexities of Italian volcanism have encouraged alternate geodynamic models for the peninsula as a whole. For instance, a rising plume beneath the western Mediterranean has been proposed in [51–53], but see [54] for an opposing view. The transition in P-residual and birefringence behaviour near the broad boundary between the Apennines and the western Alps may reflect a fixed point of attachment for the foundering Adriatic lithosphere [55], disrupting subduction flow patterns.

Alternatively, the episodic history of Apennines subduction since 30 Ma may influence anisotropy development.

Lucente and Speranza [4] argue that the Northern Apennines slab detached at 3–4 Ma from the slab further south and pivoted counter-clockwise, extending the Tuscan region and rotating the orogen. Such a model could explain the regional scale of anisotropic variations, but must be elaborated to explain the details. In particular, the weak splitting in the Tyrrhenian domain, combined with orogen-normal fast polarization near Bologna, might imply that the slab is retreating further beneath the Po River Plain, extending asthenosphere beneath the Apennines crest while leaving the upper crust in place. The development of the Ferrara arc, a buried thrust complex at the southern edge of the Po Plain, and evidence for Plio-Pleistocene uplift of the Apennine front nearby [56] may support this interpretation. Published tomographic models do not yet resolve this issue, due to resolution limitations at the base of the crust.

Complementary analyses of seismic wave speed and anisotropy, e.g., with Pn and receiver functions, will be needed to test the above hypotheses properly. Nevertheless, further analysis of a larger dataset of geographic and azimuthal dependence of anisotropic parameters [57,58] is to confirming the main result of this study, namely that the mantle flow pattern beneath the inferred Adria subduction zone departs strongly from the traditional 2-D corner flow model. Contributions from pre-existing lithospheric fabric and a 3-D sublithospheric mantle flow beneath the Northern Apennines are both likely.

## Acknowledgements

Special thanks to L. Giovani, P. Jedlička, N. Piana Agostinetti, F.P. Lucente and to all the people that helped maintain the seismographic networks. We are grateful for suggestions and recommendations of M. Fouch and anonymous referees, which improved the manuscript. J. Plomerová, V. Babuška and L. Vecsey were supported by a grant from the Grant Agency of the Academy of Sciences No. IAA3012405. V. Levin and J. Park were supported by NSF grant EAR-0208652.

## References

[1] E. Patacca, R. Sartori, P. Scandone, Tyrrhenian basin and Apenninic arcs: kinematic relations since late Tortonian times, Mem. Soc. Geol. Ital. 45 (1990) 425–451.

[2] C. Doglioni, A proposal of kinematic modelling for W-dipping subductions possible applications to the Tyrrhenian–Apennines system, Terra Nova 3 (1991) 423–434.

[3] P. Elter, M. Grasso, M. Parotto, L. Vezzani, Structural setting of the Apennine–Maghrebian thrust belt, Episodes 26 (2003) 205–211.

[4] F.P. Lucente, F. Speranza, Belt bending associated with lateral bending of subducting lithospheric slab: geophysical evidences from the Northern Apennines (Italy), Tectonophysics 337 (2001) 53–67.

[5] C. Faccenna, L. Jolivet, C. Piromallo, A. Morelli, Subduction and the depth of convection in the Mediterranean mantle, J. Geophys. Res. 107 (B2) (2003) 2099, doi:10.1029/2001JB001690.

[6] G. Selvaggi, A. Amato, Subcrustal earthquakes in the Northern Apennines (Italy): evidence for a still active subduction? Geophys. Res. Lett. 19 (1992) 2127–2130.

[7] N. D Agostino, G. Selvaggi, Crustal motion along the Eurasia–Nubia plate boundary in the Calabrian Arc and Sicily and active extension in the Messina Straits from GPS measurements, J. Geophys. Res. 109 (B11402) (2004), doi:10.1029/2004JB002998.

[8] S. Pondrelli, C. Piromallo, E. Serpelloni, Convergence vs. retreat in Southern Tyrrhenian Sea: insights from kinematics, Geophys. Res. Lett. 31 (2004) L06611, doi:10.1029/ 2003GL019223.

[9] M. Wortel, W. Spakman, Subduction and slab detachment in the Mediterranean–Carpathian region, Science 290 (2000) 1910–1917.

[10] L. Margheriti, S. Pondrelli, D. Piccinnini, N. Piana Agostinetti, F. P. Lucente, A. Amato, P. Baccheschi, L. Giovani, S. Salimbeni, J. Park, M. Brandon, V. Levin, J. Plomerová, P. Jedlicka, L. Vecsey, V. Babuška, P. Ulbricht, RETREAT seismic deployment in the Northern Apennines, Ann. Geofisica, (in press).

[11] F.P. Lucente, C. Chiarabba, G. Cimini, Tomographic constraints on the geodynamic evolution of the Italian region, J. Geophys. Res. 104 (B9) (1999) 20307–20327.

[12] C. Piromallo, A. Morelli, P wave tomography of the mantle under the Alpine–Mediterranean area, J. Geophys. Res. 108 (B2) (2003) 2099, doi:10.1029/2002JB001757.

[13] J. Plomerová, R. Arvidsson, V. Babuška, M. Granet, O. Kulhánek, G. Poupinet, J. Šílený, An array study of lithospheric structure across the Protogine Zone, Varmland, south-central Sweden; signs of a paleocontinental collision, Tectonophysics 332 (2001) 1–21.

[14] V. Babuška, J. Plomerová, L. Vecsey, M. Granet, U. Achauer, Seismic anisotropy of the French Massif Central and predisposition of Cenozoic rifting and volcanism by Variscan suture hidden in the mantle lithosphere, Tectonics 21 (2002) 1029, doi:10.1029/ 2001TC901035.

[15] G. Barruol, M. Granet, A Tertiary asthenospheric flow beneath the southern French Massif Central indicated by upper mantle seismic anisotropy and related to the West Mediterranean extension, Earth Planet. Sci. Lett. 202 (2002) 31–47.

[16] M.J. Fouch, K.M. Fischer, E.M. Parmentier, M.E. Wysession, T.J. Clarke, Shear wave splitting, continental keels, and patterns of mantle flow, J. Geophys. Res. 105 (2000) 6255–6275.

[17] Ch. Kincaid, P.S. Hall, Role of the back arc spreading in circulation and melting at subduction zones, J. Geophys. Res. 108 (B5) (2003) 2240, doi:10.1029/2001JB001174.

[18] A. Davaille, J.M. Lees, Thermal modeling of subducted plates: tear and hotspot at the Kamchatka corner, Earth Planet. Sci. Lett. 226 (2004) 293–304.

[19] S. Civello, L. Margheriti, Toroidal mantle flow around the Calabrian slab (Italy) from SKS splitting, Geophys. Res. Lett. 31 (2004) L10601, doi:10.1029/2004GL019607.

[20] V. Peyton, V. Levin, J. Park, M.T. Brandon, J. Lees, E. Gordeev, A. Ozerov, Mantle flow at a slab edge: seismic anisotropy in the Kamchatka region, Geophys. Res. Lett. 28 (2001) 379–382.

[21] V. Babuška, J. Plomerová, The lithosphere in central Europe—seismological and petrological aspects, Tectonophysics 207 (1992) 141–163.

[22] J. Plomerová, V. Babuška, R. Scarpa, Teleseismic P-residual study in the Italian region—inferences on large scale anisotropic structure of the subcrustal lithosphere, Ann. Geofis. 41 (1998) 33–48.

[23] Ch. Schmid, S. Van der Lee, D. Giardini, Delay time and shear wave splitting in the Mediterranean region, Geophys. J. Int. 159 (2004) 265–290, doi:10.1111/j.1365-246X.2004.02381.x.

[24] L. Margheriti, C. Nostro, M. Cocco, A. Amato, Seismic anisotropy beneath the Northern Apennines (Italy) and its tectonic implications, Geophys. Res. Lett. 23 (1996) 2721–2724.

[25] L. Margheriti, L. Lucente, S. Pondrelli, SKS splitting measurements in the Apenninic–Tyrrhenian domain (Italy) and their relation with lithospheric subduction and mantle convection, J. Geophys. Res. 108 (B4) (2003) 2218, doi:10.1029/2002JB001793.

[26] V. Levin, L. Margheriti, J. Park, A. Amato, Anisotropic seismic structure of the lithosphere beneath the Adriatic coast of Italy constrained with mode-converted body waves, Geophys. Res. Lett. 29 (22) (2002) 2058, doi:10.1029/2002GL015438.

[27] F.P. Lucente, L. Margheriti, C. Piromallo, G. Barruol, Seismic anisotropy reveals the long route of the slab through the western–central Mediterranean mantle, Earth Planet. Sci. Lett. 241/3-4 (2006) 517–529, doi:10.1016/j.epsl.2005.10.041.

[28] J. Park, V. Levin, Seismic anisotropy: tracing plate dynamics in the mantle, Science 296 (2002) 485–489.

[29] G. Smith, D.A. Wiens, K.M Fischer, L.M. Dorman, S.C. Webb, J.A. Hildebrand, A complex pattern of mantle flow in the Lau backarc, Science 292 (2001) 713–716.

[30] Ch.E. Hall, K.M. Fischer, E.M. Parmentier, The influence of plate motions on three-dimensional back-arc mantle flow and shear wave splitting, J. Geophys. Res. 205 (2000) 28009–28033.

[31] C.A. Currie, J.F. Cassidy, R.D. Hyndman, M.G. Bostock, Shear wave anisotropy beneath the Cascadia subduction zone and western North America craton, Geophys. J. Int. 157 (2004) 341–353.

[32] M.J. Fouch, P.G. Silver, D.R. Bell, J.N. Lee, Small-scale variations in seismic anisotropy near Kimberley, South Africa, Geophys. J. Int. 157 (2004) 764–774.

[33] E.R. Klosko, F.T. Wu, H.J. Anderson, D. Eberhard-Phillips, T.V. McEvilly, E. Audoine, M.K. Savage, K.R. Gledhill, Upper mantle anisotropy in the New Zealand, Geophys. Res. Lett. 26 (1999) 1497–1500.

[34] E. Pera, D. Mainprice, L. Burlini, Anisotropic seismic properties of the upper mantle beneath the Torre Alfina area (Northern Apennines, central Italy), Tectonophysics 370 (2003) 11–30.

[35] P.G. Silver, W.W. Chan, Shear wave splitting and subcontinental mantle deformation, J. Geophys. Res. 96 (1991) 16429–16454.

[36] J. Šílený, J. Plomerová, Inversion of shear-wave splitting parameters to retrieve three-dimensional orientation of anisotropy in continental lithosphere, Phys. Earth Planet. Inter. 95 (1996) 277–292.

[37] E. Sandvol, T. Hearn, Bootstrapping shear-wave splitting errors, Bull. Seismol. Soc. Am. 85 (1994) 1971–1977.

[38] G. Rumpker, A. Tommasi, M.J. Kendall, Numerical simulations of depth-dependent anisotropy and frequency-dependent wave propagation, J. Geophys. Res. 104 (1999) 23141–23153.

[39] I. Matcham, M.K. Savage, K.R. Gledhill, Distribution of seismic anisotropy in the subduction zone beneath the Wellington region, New Zealand, Geophys. J. Int. 140 (2000) 1–10.

[40] K. Marson-Pidgeon, M.K. Savage, Frequency-dependent anisotropy in Wellington, New Zealand, Geophys. Res. Lett. 24 (1997) 3297–3300.

[41] W. Menke, V. Levin, A waveform-based method for interpreting SKS splitting observations, with application to one and two layer anisotropic Earth models, Geophys. J. Int. 154 (2003) 379–392.

[42] J. Plomerová, Seismic anisotropy in tomographic studies of the upper mantle beneath southern Europe, Ann. Geofis. 40 (1997) 111–121.

[43] V. Babuška, J. Plomerová, J. Šílený, Models of seismic anisotropy in the deep continental lithosphere, Phys. Earth Planet. Inter. 78 (1993) 167–191.

[44] V. Babuška, J. Plomerová, J. Šílený, Large-scale oriented structures in the subcrustal lithosphere of central Europe, Ann. Geophys. 2 (1984) 649–662.

[45] K.C. Creager, T.H. Jordan, Slab penetration into the lower mantle, J. Geophys. Res. 89 (1984) 3031–3049.

[46] V. Levin, W. Menke, A. Lerner-Lam, Seismic anisotropy in the northeastern US as a source of significant teleseismic P traveltime anomalies, Geophys. J. Int. 126 (1996) 593–603.

[47] A. Levshin, M.H. Ritzwoller, M.P. Barmin, A. Villaseñor, C.A. Padgett, New constraints on the arctic crust and uppermost mantle: surface wave group velocities, $P_n$, and $S_n$, Phys. Earth Planet. Inter. 123 (2001) 185–204.

[48] G. Mele, A. Rovelli, D. Seber, T.M. Hearn, M. Barazangi, Compressional velocity structure and anisotropy in the uppermost mantle beneath Italy and surrounding regions, J. Geophys. Res. 103 (1998) 12529–12543.

[49] N. Piana Agostinetti, F.P. Lucente, G. Selvaggi, M. Di Bona, Crustal structure and Moho geometry beneath the Northern Apennines (Italy), Geophys. Res. Lett. 29 (20) (2002) 1999, doi:10.1029/2002GL015109.

[50] G. Mele, E. Sandvol, Deep crustal roots beneath the Northern Apennines inferred from teleseismic receiver functions, Earth Planet. Sci. Lett. 211 (2003) 69–78.

[51] R. Vollmer, Rb–Sr and U–Th–Pb systematics of alkaline rocks: the alkaline rocks from Italy, Geochim. Cosmochim. Acta 40 (1976) 283–295.

[52] K. Bell, F. Castorina, G. Lavecchia, G. Rosatelli, F. Stoppa, Is there a mantle plume beneath Italy, EOS Trans. AGU 85 (541) (2002) 546–547.

[53] G. Lavecchia, P. Boncio, N. Creati, F. Brozzetti, Some aspects of the Italian geology not fitting with a subduction scenario, J. Virtual Explorer 10 (2003) 1–42.

[54] A. Peccerillo, M. Lustrino, Compositional variations of Plio-Quaternary magmatism in the circum-Tyrrhenian area: deep- vs. shallow-mantle processes, in: G.R. Foulger, J.H. Natland, D.C. Presnall, D.L. Anderson (Eds.), Plates, Plumes and Paradigms, Geol. Soc. Am. Spec. Pap., 388, 2005, pp. 421–434.

[55] H. Laubscher, G.C. Biella, R. Cassinis, R. Gelati, A. Lozej, S. Scarascia, I. Tabacco, The collisional knot in Liguria, Geol. Rundsch. 81 (1992) 275–289.

[56] A. Castellarin, Alps-Apennines and Po Plain-frontal Apennines relations, in: G.B. Vai, I.P. Martini (Eds.), Anatomy of an Orogen: the Apennines and Adjacent Mediterranean Basins, Kluwer Academic, Amsterdam, 2001, pp. 177–196.

[57] S. Salimbeni, S. Pondrelli, L. Margheriti, A. Amato, J. Plomerová, J. Park, M. Brandon, V. Levin, RETREAT Seismology Team, Seismic Anisotropy in the upper mantle around the Northern Apennines: results of RETREAT's project, Geophys. Res. Abstr. 8 (04143) (2006) SRef-ID: 1607-7962/gra/EGU06-A-04143.

[58] V. Levin, J. Park, L. Margheriti, F.P. Lucente, Structure and texture of the upper mantle beneath Northern Apennines: evidence from quasi-Love waves, Geophys. Res. Abstr. 8 (05413) (2006) SRef-ID: 1607-7962/gra/EGU06-A-05413.